12WCEE 2000

STRUCTURAL RESPONSE OF RC PIER UNDER VERTICAL EARTHQUAKE SHOCK

Nobutaka ISHIKAWA[1], Masuhuhiro BEPU[2], Satoshi KATSUKU[3], Ayaho MIYAMOTO[4] And Klaus BRANDES[5]

SUMMARY

This paper presents both experimental and analytical studies for the reappearance of a circumferential crack in reinforced concrete (RC) piers during the Hyogoken-Nanbu Earthquake. First, a newly developed push-up impact test was performed for a RC pier model. The failure of circumferential crack was occurred in the specimen and its failure process was taken by the high-speed video. Second, the multi degree of freedom model analysis is adopted in order to examine the occurrence mechanism of a circumferential crack. Third, a two dimensional FEM is developed to investigate in detail the failure process of a RC pier model under vertical earthquake shock. Finally, an actual RC pier is analyzed and the input earthquake velocity is estimated from the viewpoint of the tensile limit strain of concrete.

INTRODUCTION

A circumferential crack as shown in Photo 1 was observed in many RC piers in the 1995 Hyogoken-Nanbu earthquake in Japan [1]. It is generally said that this failure may be caused by flexural crack due to the horizontal ground vibration. However, many witness reported that they were shocked by push-up motion at the beginning of the earthquake [2]. These facts suggested that the impulsive vertical motion in the earthquake possibly induced the circumferential crack of RC piers [3, 4].

This paper presents both experimental and analytical approaches for the reappearance of a circumferential crack phenomenon of the RC pier[4, 5]. First, a new push-up impact apparatus was developed and the vertical motion was applied to the RC pier model. Second, the occurrence mechanism of a circumferential crack of RC pier is investigated by using the multi degree of freedom model. Third, a two dimensional FEM is also developed in order to examine the failure process of a RC pier in detail. Finally, an actual RC pier is analyzed by a single degree of freedom system in order to examine the effect of the upper structure weight and the input vertical velocity. As the numerical results, the input vertical earthquake motion is predicted by exceeding the tensile limit strain of concrete, i.e., the occurrence of a circumferential crack.

2. EXPERIMENTAL PROCEDURE

2.1 Test Instrumentation :

Figure 1 shows the newly developed push-up impact apparatus which is composed of input and output actuators connected by a rubber pipe as shown in Photo 2. Filling the entire apparatus with mechanical oil, the input actuator is compressed quickly by the hydraulic high speed loading machine with about 400cm/s, then the output actuator goes up and stopped impulsively. Therefore, the specimen on the base plate of output actuator is also thrust up and stopped suddenly.

[1] *Dept of Civil Eng, National Defense Academy, Yokusuka, JAPAN. e-mail ishikawa@cc.nda.ac.jp*
[2] *Dept of Civil Eng, National Defense Academy, Yokusuka, JAPAN.*
[3] *Dept of Civil Eng, National Defense Academy, Yokusuka, JAPAN.*
[4] *Faculty of Engineering, Yamaguchi University, Ube, JAPAN*
[5] *Bundesanstalt fiir Materrialpriifung (BAM), Berlin, GERMANY*

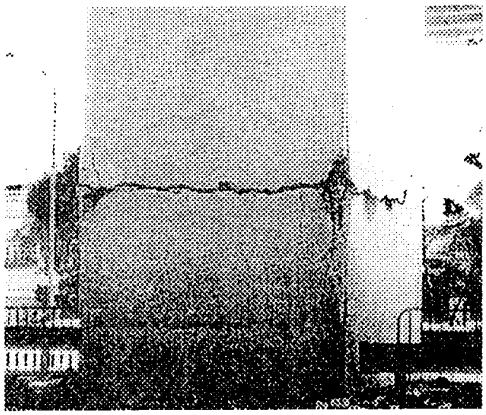

Photo 1 : An example of circumferential crack of RC pier

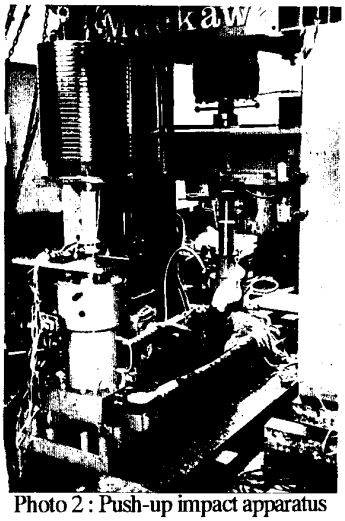

Photo 2 : Push-up impact apparatus

Table 1: Mix proportion of concrete

Compressive Strength	34.3N/mm^2	Water	174kg/m^3
Slump	10cm	Cement	305kg/m^3
Air	1.0%	Expansion agent	15kg/m^3
Water-cement ratio	54%	Fine aggregate	1021kg/m^3
Sand percentage	55%	Coarse Aggregate	852kg/m^3

Table 2: Results of steel material test

Classify	Tensile strength (Average,N/mm^2)	Elongation (Average, %)
M10 Bolt	536. 7	12. 7
D6 Steel bar	558	32

※Yield points were not recognized

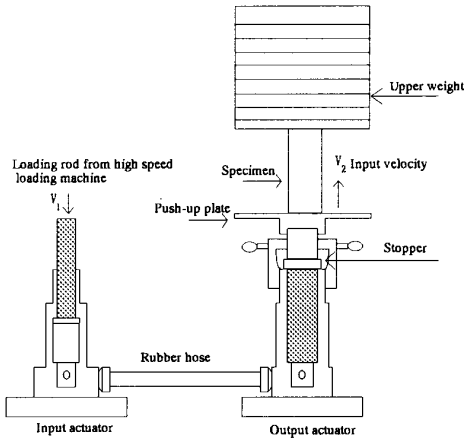

Figure 1 : Push-up impact apparatus

2.2 Specimens :

Assuming that an actual RC pier is 10m in height and has circular cross section which is 3m in diameter, four types specimens which have various scales and main reinforcements are used as shown in fig.2, i.e., Type A : 1/30 scale, only upper and lower part sections are reinforced by a bolt, Type B : 1/30 scale model which is reinforced by a bolt, Type C : 1/30 scale model which is reinforced by a bolt and by four D6 reinforcing bars cut off at half in height, Type D : 1/50 scale model is reinforced by a bolt. M10 bolt is used as a reinforcing bar because of restriction for fix condition of specimen. The surcharge weight at the top of specimen is 4.9kN and it makes 62kPa surcharge stress in the specimen. Tables 1 and 2 show the mix proportion of concrete and the results of steel material test, respectively.

2.3 Measurement :

Measurement items are shown in fig.3. The accelerations and displacements of surcharge weight and base plate were measured by an acceleration transducer and a displacement sensor,

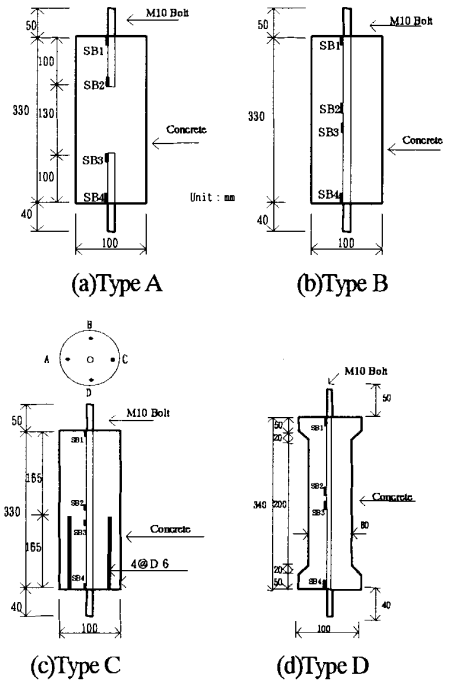

Figure 2 : Specimens and strain gauges of reinforcing bar

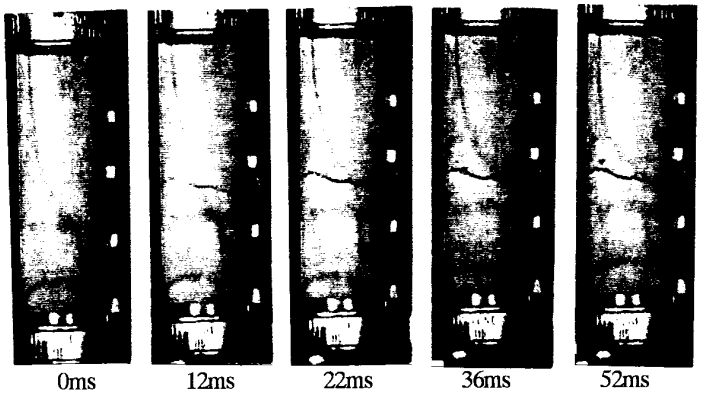

Photo3 : Circumferential crack by high speed video

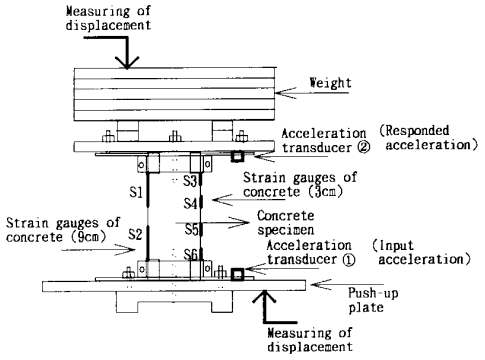

Figure 3: Measuring points

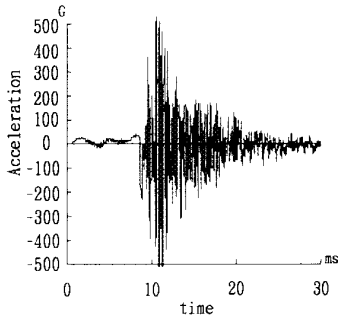

(a) Input acceleration-time relation

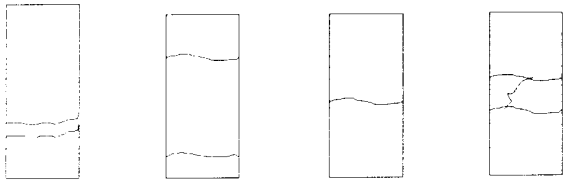

Figure 5 : Failure modes

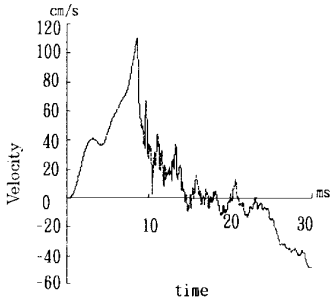

(a) Input velocity-time relation

Figure 4 : Input acceleration ($\ddot{\phi}$) and input velocity($\dot{\phi}$)

respectively. The strains of interior reinforcing bars and the concrete were measured using strain gauges as shown in figs. 2 and 3, respectively.

3 EXPERIMENTAL RESULTS AND CONSIDERATIONS

3.1 Input Acceleration and Velocity:

Figures 4 (a) and (b) show the input acceleration and velocity-time relations obtained in the test, respectively. It is found from fig. 4 (a) that the input acceleration is applied to the specimen as the positive value until 8ms and shows instantly large vibrating values, because the output actuator stopped suddenly. It is also noted from fig.4 (b) that the input velocity goes up until 110cm/s at the 8ms and goes down suddenly at the time 10ms.

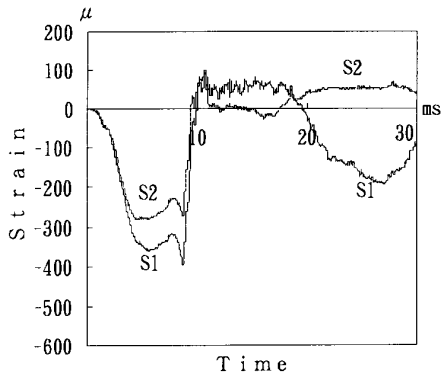

Figure 6 : Concrete strain-time relation

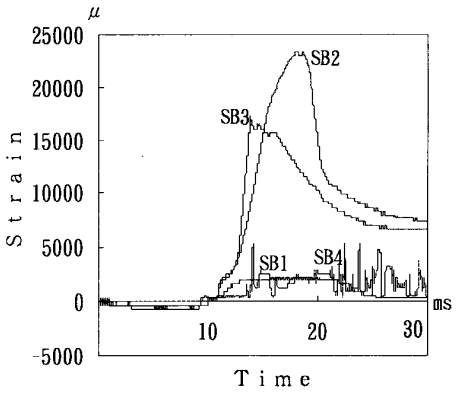

Figure 7 : Bolt strain-time relation

3.2 Failure Modes :

Photo 3 shows the progressive process of a circumferential crack in Type C taken by a high speed video. A single circumferential crack occurs at the place of supplement reinforcement bar cut off point of Type C. Figure 5 shows the typical failure modes of type A, B, C and D. Type A belongs to the separate failure mode. The failure position is the cut off point of upper or lower reinforcing bolt. Because, the stiffness in axial direction varies and the reinforcing effect is lost at the cut off point. Type B is the failure mode in which two cracks are occurred at the middle point. This might be the reason why the second crack was occurred in the weak concrete section due to the tension force of bolt after the occurrence of the first crack. Type C is always the failure mode of one circumferential crack at the middle of specimen which is around the cut off point. This may be caused by the stress concentration at the varying section of stiffness. Type D belongs to the failure mode in which both circumferential cracks and axial cracks are occurred. This may be the reason why the unbalanced loading of upper weight may make specimen sway a little at the time of stopping.

3.3 Strain-time relations :

The concrete strain (S1, S2) -time relation of Type C is shown in fig.6. From this figure, the maximum compressive strain was 400μ (S1) at 8ms (specimen started stopping at this time), and after that, the compressive strain was transformed into the tensile strain quickly. In this case, one circumferential crack was occurred in the center of specimen at 12ms as shown in Photo 3 and concrete strain (S1, S2) showed the maximum tensile strain about 100μ which does not exceed the limit tensile strain (150μ). Because S1 and S2 strains are derived from the cut off position. On the contrary, S4 strain exceeds the limit tensile strain (150μ) as shown in fig. 10. The bolt strain (SB1, SB2, SB3, SB4)-time relation is shown in fig.7. After occurring of circumferential crack, the middle position strain (SB2, SB3) showed large tensile strain and the maximum strain value was 2.4% (SB2). Upper and lower position strains (SB1, SB4) showed very small values as compared with the middle strain (SB2, SB3).

4. DYNAMIC ANALYSIS BY MULTI DEGREE OF FREEDOM SYSTEM AND FEM

4.1 Analytical Model of Multi Degree of Freedom System :

The specimen is modeled to the multi degree of freedom model as shown in fig. 8. The spring constants of concrete, bolt and steel bar are determined by the material properties and the cross sectional areas, respectively. Therefore, the governing equation is derived from the dynamic equilibrium condition as shown in fig. 9 as follows :

$$\mathbf{M}\ddot{\mathbf{u}} + \mathbf{C}\dot{\mathbf{u}} + \mathbf{K}\mathbf{u} = -\mathbf{M}\ddot{\phi} \qquad (1)$$

where $\mathbf{M}$ is mass matrix, $\mathbf{C}$ is damping matrix, $\mathbf{K}$ is stiffness matrix, $\ddot{\phi}$ is input vertical acceleration vector and $\ddot{\mathbf{u}}$, $\dot{\mathbf{u}}$, $\mathbf{u}$ are acceleration, velocity, displacement vectors, respectively.

Table 3. Input data of analysis

Members	9	Limit compressive strain of concrete ($\times 10^{-6}$)	2200
Masses	10	Crack strain of concrete ($\times 10^{-6}$)	150
Damping constant (%)	7	Yield strain of steel ($\times 10^{-6}$)	1400

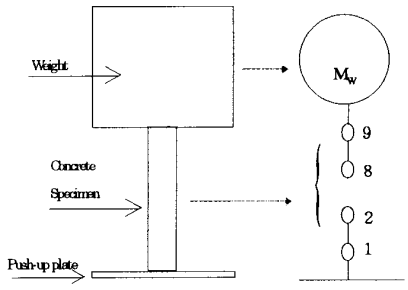

(a) Specimen (b)Analytical model

Figure 8 : Analytical model of specimen

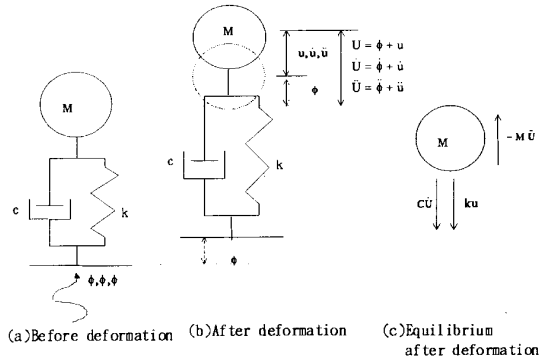

(a)Before deformation (b)After deformation (c)Equilibrium after deformation

Figure 9 : Equilibrium at mass

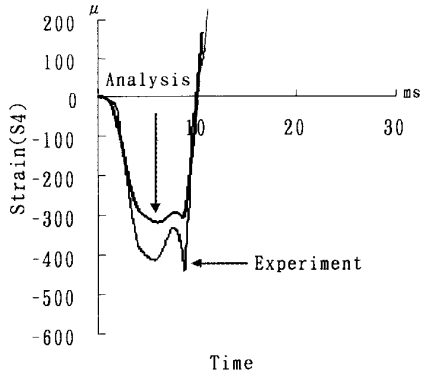

Figure 10 : Comparison between analysis and experimental results

By solving Eq. (1) using Newmark β method, the displacement at each mass is found and the strain between masses is also obtained by the difference of displacements.

4.2 Computational Results :

Input data used in the analysis is shown in Table 3 and the input acceleration is shown in fig. 4 (a). Figure 4 (b) shows the input velocity-time relation which integrates the acceleration-time relation in fig. 4 (a). As an example of simulations, Figure 10 shows the computational and experimental results of concrete strain-time relation at the measuring point of S4 (See fig. 3). From this figure, the analytical result shows good agreement with experimental one in wave shape and period.

4.3 Occurrence Mechanism of a Circumferential Crack :

On the basis of analytical results, the occurrence mechanism of a circumferential crack may be estimated as follows :

Figures 11 (a) and (b) show the input characteristics model (acceleration, velocity, displacement) and the behavior of a specimen corresponding to the input characteristics, respectively. Input velocity rises up proportionally from t=0 to $t=t_1$ and instantly drops 0 from $t=t_1$ to $t=t_2$. Therefore, the input acceleration has a small positive value from t=0 to $t=t_1$, and a large negative value from $t=t_1$ to $t=t_2$. The inertia force ($F = -M\ddot{\phi}$) is acting to the upper mass and, therefore, the column becomes to be subjected to the large tensile force from $t=t_1$ to $t=t_2$ as shown in fig.11 (b). Consequently, a circumferential crack will be naturally occurred in the concrete specimen. This occurrence mechanism of a circumferential crack corresponds to the strain-time relation in fig. 10.

4.4 Simulation by FEM :

The multi degree of freedom model can describe the principle feature of the occurrence mechanism of a circumferential crack. However, this model can not simulate in detail the effect of cut-off point at which the circumferential fracture is occurred. Therefore, a finite element method (FEM) is developed in order to examine in more detail the behavior of a specimen. The

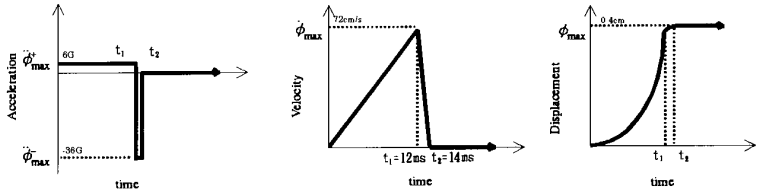

(a)Input characteristics model

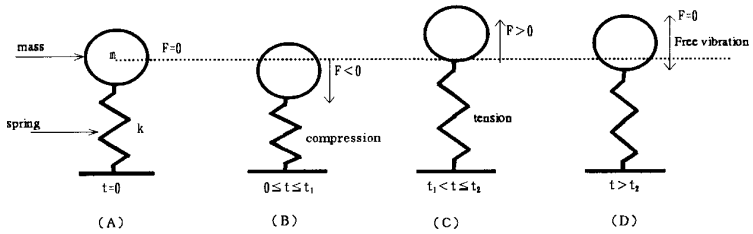

(b) Behavior of specimen ($\mathbf{F}=-\mathbf{M}\ddot{\phi}$: Inertia force)

Figure 11 : occurring mechanism of circumferential crack

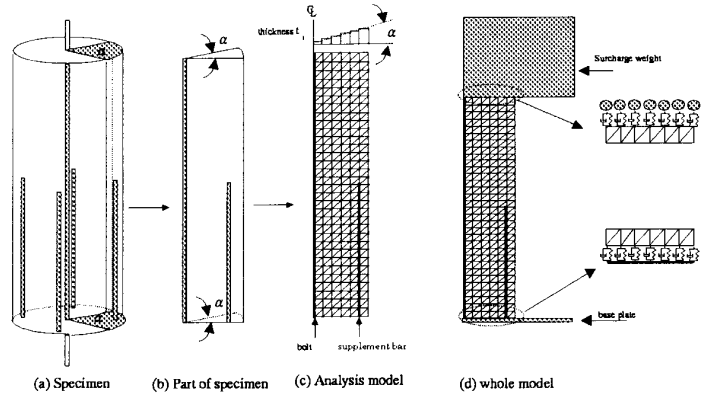

Figure 12 : Analytical model

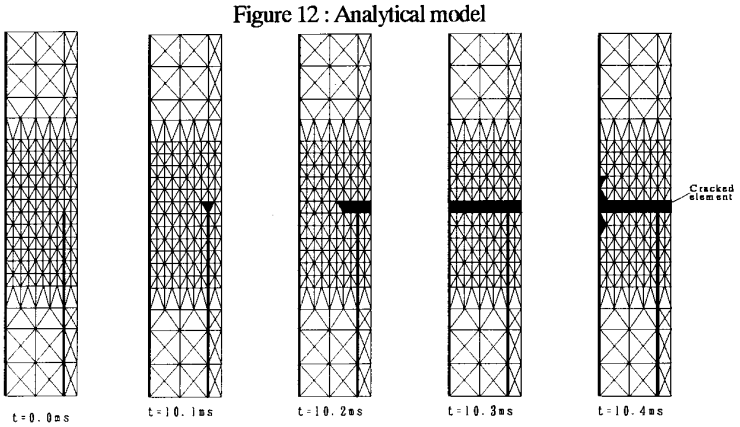

Figure 13 : Cracked element progression

plane strain triangular element model is adopted and the radial sliced part of the specimen which contains one supplement reinforcement bar is also modeled as shown in fig. 12. Figure 13 shows the progressive process of cracked elements. The initiated cracked element appeared at the top of cut-off supplement reinforcement bar (t=10.1ms) and the cracked element progresses horizontally to the free surface. After circumferential crack is completed, the cracked element occurs along the reinforcement bar.

Table4 : Properties of actual RC pier

Young's modulus	28kN/mm^2
Cross sectional area	1.156$\times 10^5$cm^2

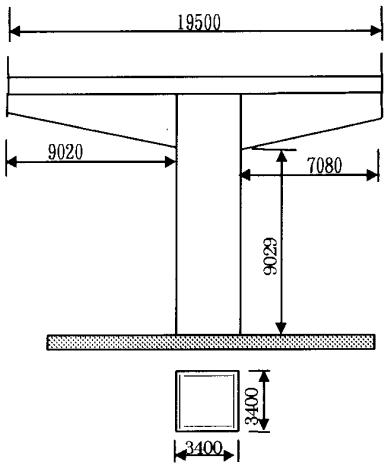

Figure 14 : Actual RC pier

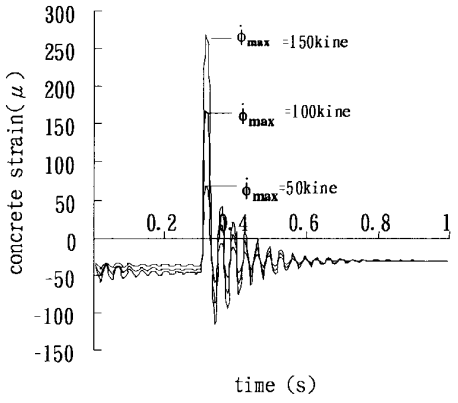

Figure 16 : Effect of input velocity (at W=9800kN)

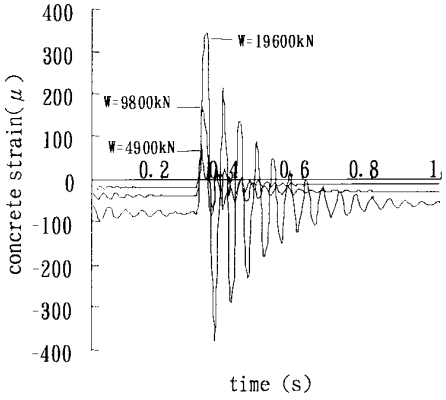

Figure 15 : Effect of upper weight (at $\dot{\phi}_{max}$ =100kyne)

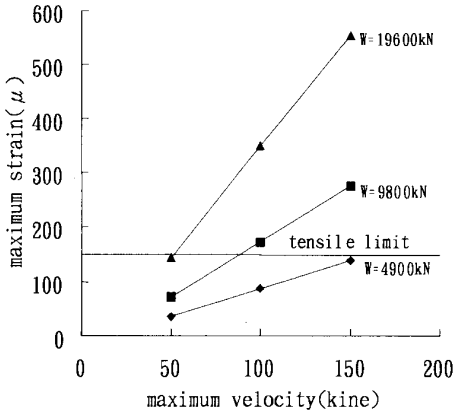

Figure 17 : Maximum tensile strain -maximum velocity relation

5. APPLICATION TO THE ACTUAL RC PIER

The actual RC pier as shown in fig. 14 and Table 4 is analyzed by using a single degree of freedom system in order to examine the effects of upper structure weight and the input velocity. Herein, the RC pier has no cut-off point and about 1.4% reinforcement ratio. The input velocity model is used as shown in fig. 11 (b) with t_1=0.3sec and t_2=0.03sec changing the maximum velocity.

5.1 Effect of Upper Structure Weight :

In order to examine the effects of upper structure weight and input velocity, three kinds of weights (4900kN, 9800kN,19600kN) and three kinds of maximum velocities (50kine, 100kine, 150kine) were adopted in the analysis. Figure 15 shows the concrete strain-time relation changing the upper weight at the constant velocity ($\dot{\phi}_{max}$ =100kine). It is found that the concrete strain is

increased remarkably as the increase of upper weight. It is also noted that the strain is changed suddenly from compression to tension at the time t=0.3sec, and, therefore, the tensile strain exceeds about 150μ of the limit tensile strain.

5.2 Effect of Input Velocity :

Figure 16 shows the concrete strain-time relation changing the input velocity at the constant weight W=9800kN. It is found that the tensile strain does not exceed the limit strain 150μ in case of velocity $\dot{\phi}_{max}$ =50kine, but exceeds in case of over velocity $\dot{\phi}_{max}$ =100kine.

Figure 17 shows the relationship between the maximum response strain and the maximum input velocity. It is noted that the tensile response strain does not exceed the limit strain 150μ in case of weight W=4900kN, but exceeds in cases of W=19600kN at over $\dot{\phi}_{max}$ =50kine and W=9800kN at over $\dot{\phi}_{max}$ =80kine. This predicts that the circumferential crack will be occurred in such conditions.

6. CONCLUSIONS

The following conclusions are derived from this study.

1. The circumferential crack was reappeared by using the newly developed push-up impact apparatus.
2. Computational results by the multi degree of freedom model method and the FEM shows good agreements with experimental ones. The FEM could examine the failure process of RC pier model in detail.
3. It was found that the large positive inertia force will cause large tensile force and a circumferential crack in RC pier
4. It was predicted that a circumferential crack might be occurred in cases of W=19600kN at over $\dot{\phi}_{max}$ =50kine and W=9800kN at over $\dot{\phi}_{max}$ =80kine.

7. REFERENCES

1. Sonoda,. K., Kobayashi, H., (1997), "On impact-like failure of reinforced concrete structures by Hyogo-ken Nanbu Earthquake (Kobe, 1995), Earthquake Resistant Engineering Structures, Computational Mechanics Publications, pp.693-704.
2. Sonoda, K., Kobayashi, H., (1997), " On the witness of vertical earthquake shock - Hyogoken Nanbu Earthquake-", The Memories of Faculty of Engineering, Special Issue of Earthquake Disaster, January , pp.187-270.
3. Takemiya, H., Goda, K. and Hriuchi, S., (1996), " Transient response of structures and ground due to impulsive seismic loading", Proc. of the First Asia-Pacific Conference on Shock & Impact Loads on Structures, Singapore, January, pp.445-452.
4. Elnashai, A. S. and Papazoglou, A., (1995), " Vertical Earthquake Ground Motion ; Evidence, Effects and Simplified Analysis Procedures", ESEE Research Report 95/6, Imperial College, London, Dec, pp.1-45.
5. Beppu, M., Katsuki, S., Ishukawa, N. and Miyamoto, A., (1997), " An experimental study on circumferential crack of RC pier model by push-up impact test", Proc. of JSCE, No. 577/I-41, Oct, pp.165-180.
6. Ishikawa, N., Beppu, M., Katsuki, S. and Miyamoto, A. (1999), " Effect of steel iacket reinforcement of RC pier model under impulsive vertical motion", Earthquake Resistant Engineering Structures Ⅱ, WIT press, pp.13-22.